Journal of Cerebral Blood Flow & Metabolism (2014) 34, 325–331

www.jcbfm.com

ORIGINAL ARTICLE

Microvascular sprouting, extension, and creation of new capillary connections with adaptation of the neighboring astrocytes in adult mouse cortex under chronic hypoxia

Kazuto Masamoto[1,2], Hiroyuki Takuwa[2], Chie Seki[2], Junko Taniguchi[2], Yoshiaki Itoh[3], Yutaka Tomita[3], Haruki Toriumi[3], Miyuki Unekawa[3], Hiroshi Kawaguchi[2], Hiroshi Ito[2], Norihiro Suzuki[3] and Iwao Kanno[2]

The present study aimed to determine the spatiotemporal dynamics of microvascular and astrocytic adaptation during hypoxia-induced cerebral angiogenesis. Adult C57BL/6J and Tie2-green fluorescent protein (GFP) mice with vascular endothelial cells expressing GFP were exposed to normobaric hypoxia for 3 weeks, whereas the three-dimensional microvessels and astrocytes were imaged repeatedly using two-photon microscopy. After 7 to14 days of hypoxia, a vessel sprout appeared from the capillaries with a bump-like head shape (mean diameter 14 μm), and stagnant blood cells were seen inside the sprout. However, no detectable changes in the astrocyte morphology were observed for this early phase of the hypoxia adaptation. More than 50% of the sprouts emerged from capillaries 60 μm away from the center penetrating arteries, which indicates that the capillary distant from the penetrating arteries is a favored site for sprouting. After 14 to 21 days of hypoxia, the sprouting vessels created a new connection with an existing capillary. In this phase, the shape of the new vessel and its blood flow were normalized, and the outside of the vessels were wrapped with numerous processes from the neighboring astrocytes. The findings indicate that hypoxia-induced cerebral angiogenesis provokes the adaptation of neighboring astrocytes, which may stabilize the blood–brain barrier in immature vessels.

Journal of Cerebral Blood Flow & Metabolism (2014) **34,** 325–331; doi:10.1038/jcbfm.2013.201; published online 20 November 2013

Keywords: cerebral microcirculation; cranial window; neuron–glia–vascular unit; two-photon laser-scanning fluorescence microscopy; vascular plasticity

INTRODUCTION

The blood–brain barrier (BBB), a unique functional feature of the brain vasculature, forms an interface between the systemic blood circulation and the central nervous system. The major role of the BBB is to control the central nervous system microenvironment to maintain neural signaling through transport barriers in the endothelial junctions with perivascular astrocytes[1] (for a review see Abbott *et al*[2]). In an Alzheimer's disease mouse model, anticipation of an increase in BBB permeability behind the pathogenesis was found.[3] A persistent disruption of the BBB is causally related to progression of neuronal dysfunction, as in temporal lobe epilepsy.[4] These findings indicate that an alteration in the BBB participates in the pathogenesis and progression of neurodegenerative disorders.[5–7]

Hypoxia is a strong stimulant that threatens the health of the neurovascular unit. In response to continuous exposure to hypoxia, several angiogenesis-promoting factors are upregulated, such as hypoxia-inducible factor-1α and vascular endothelial growth factor in cortical neurons and astrocytes.[8,9] Upregulation of angiopoietin-2, fibronectin, and $\alpha5\beta1$ integrin was also observed in cortical vascular endothelial cells after exposure to chronic hypoxia.[10,11] In accordance with these molecular events, an increase in microvascular density was shown in rats and mice exposed to chronic hypoxia.[12,13] Furthermore, a recent *in vivo* microscopic study has revealed that the brain microvasculature has morphologic 'plasticity' that promote cerebral angiogenesis in adult mice.[14] However, the spatiotemporal dynamics of hypoxia-induced cerebral angiogenesis remain largely unknown in *in vivo* brains, such as for sequences of vessel sprouting, endothelial cell migration, tube formation, creation of new vessel connections, and stabilization of newly formed vessels.[15–17] Specifically, the cellular interplay in regulating the integrity of the BBB during cerebral angiogenesis is an open question.[18,19]

In our previous studies, longitudinal *in vivo* imaging methods for microvessels and astrocytes were established using either confocal or two-photon microscopy in a living mouse cortex through closed cranial window.[20–22] With these imaging systems, we found a disruption of the BBB after focal ischemia but not during chronic hypoxia under which the parenchymal capillaries were significantly dilated.[20–22] Because the BBB is regulated by interactions between multiple cells, such as neuron, glia, and vascular cells, these morphologic and functional changes in the microvasculature must be made collaboratively with the perivascular cells, such as astrocytes; thus, a further understanding of the cellular interactions between angiogenic endothelial cells and the neighboring astrocytes is needed.

[1]Brain Science Inspired Life Support Research Center, University of Electro-Communications, Chofu, Tokyo, Japan; [2]Molecular Imaging Center, National Institute of Radiological Sciences, Inage, Chiba, Japan and [3]Department of Neurology, School of Medicine Keio University, Shinjuku, Tokyo, Japan. Correspondence: Dr I Kanno, Molecular Imaging Center, National Institute of Radiological Sciences, 4-9-1 Anagawa, Inage, Chiba 263-8555, Japan.
E-mail: kanno@nirs.go.jp
This study was partially supported by JSPS KAKENHI (No. 25750400) for KM and a grant from the Ministry of Health, Labor and Welfare (MHLW), Japan and JSPS KAKENHI (No. 24659578) for IK.
Received 28 June 2013; revised 16 October 2013; accepted 23 October 2013; published online 20 November 2013

In the present study, we focused on the angiogenic responses of the microvasculature and the neighboring astrocytes in *in vivo* mouse cortex under chronic hypoxia. To characterize the spatiotemporal dynamics of the morphologic adaptations during hypoxia-induced cerebral angiogenesis, the three-dimensional microvessels and astrocytes were imaged before and during 3 weeks of hypoxia using repeated two-photon microscopy. Genetically engineered mice with vascular endothelial cells expressing green fluorescent protein (GFP) were used to determine the angiogenic response, and sulforhodamine 101 (SR101) was used to fluorescently label blood plasma (i.e., perfused microvessels) and astrocytes.[21,23] This dye was also used to monitor a leakage of the BBB during the imaging experiments *in vivo*.[24]

MATERIALS AND METHODS

Animals

Animal use and experimental protocols were approved by the Institutional Animal Care and Use Committee in the National Institute of Radiological Sciences (Inage, Chiba, Japan). Seven STOCK Tg(Tie2-GFP) 287Sato/J mice (8 to 20 weeks old, male and female; The Jackson Laboratory, Bar Harbor, ME, USA) with vascular endothelial cells expressing GFP[25,26] and four male C57BL/6J mice (8 to 12 weeks old; Japan SLC, Shizuoka, Japan) were used for the experiments following the institutional guideline. There were no apparent differences between these two species in their hypoxia response; thus, the results for both animals were included in the analysis.

Two-Photon Microscopy

The animals were anesthetized with isoflurane (2% to 3%), and a closed cranial window (a cover glass 3 to 4 mm in diameter) was made over the left parietal cortex at least 1 week before the imaging experiments.[20] For the imaging experiments, the animals were anesthetized with isoflurane (2% to 3% for induction and 1% for the experiments). An intraperitoneal injection (8 μL/g body weight) of SR101 (MP Biomedicals, Irvine, CA, USA) dissolved in saline (5 to 10 mmol/L) was administered,[21] and then the animals were placed on a custom-made apparatus fixed on the stage of the microscope.[27] The SR101 is a small biocompatible molecule that has been used to stain microvessels and astrocytes *in vivo*,[21,23] and also used to measure the permeability of the BBB.[24] For the Tie2-GFP mice, concurrent imaging of the microvessels and astrocytes was performed using band-pass filters of 525/50 nm (for GFP) and 610/75 nm (for SR101), respectively, and two-photon microscopy (TCS-SP5MP; Leica Microsystems GmbH, Wetzlar, Germany) excited with a 900-nm Ti:sapphire laser (MaiTai HP, Spectra-Physics, Santa Clara, CA, USA). For the C57BL/6J mice, the microvessels and astrocytes were imaged with a single-channel detector using a band-pass filter of 610/75 nm (for SR101).

The image consisted of 1,024 $\times$ 1,024 pixels, and the in-plane pixel size was 0.25 to 0.45 μm or 1.8 μm with a $\times$20 or $\times$5 objective lens, respectively. A series of z-stack images were acquired with a step size of 2.5 to 5.0 μm up to a depth of 300 to 800 μm from the cortical surface. For follow-up imaging, the pattern of the cortical surface vasculature imaged with confocal microscopy (see Figure 1A) was used to identify the previously measured locations to track the same microvessels and astrocytes. In each animal, 8 to 11 locations were imaged in the peripheral regions of the middle cerebral artery and anterior cerebral artery territories.[21] The total time for taking all of the images for each experiment was approximately 3 hours. During this time period, the animals breathed room air with a mixture of 1% isoflurane, and the rectal temperature was maintained at 37°C to 38°C.

Hypoxia Exposure

The animals were placed in a custom-made hypoxia chamber (140 mm $\times$ 200 mm $\times$ 70 mm).[22] The oxygen concentration in the chamber was monitored with an oxygen sensor (OC-6B; Komyo Rikagaku Kogyo KK, Kawasaki, Japan) and maintained at 8% to 9% with a continuous infusion (0.05 to 0.08 L/min) of a moistening gas mixture of oxygen and nitrogen, blended with a gas mixture device (Kofloc GB-2C; Kojima Instrument, Kyoto, Japan). This level of hypoxia decreased the animal's body weight by 20% during 21 days of exposure and increased the hematocrit from 0.35 to 0.69 after 21 days of hypoxia.[28] Nevertheless, the cortical neural activity remained unchanged compared with prehypoxia.[28] During the entire period of hypoxia experiments, the animal was kept in the chamber except for weekly cleaning of the chamber and the imaging experiments.

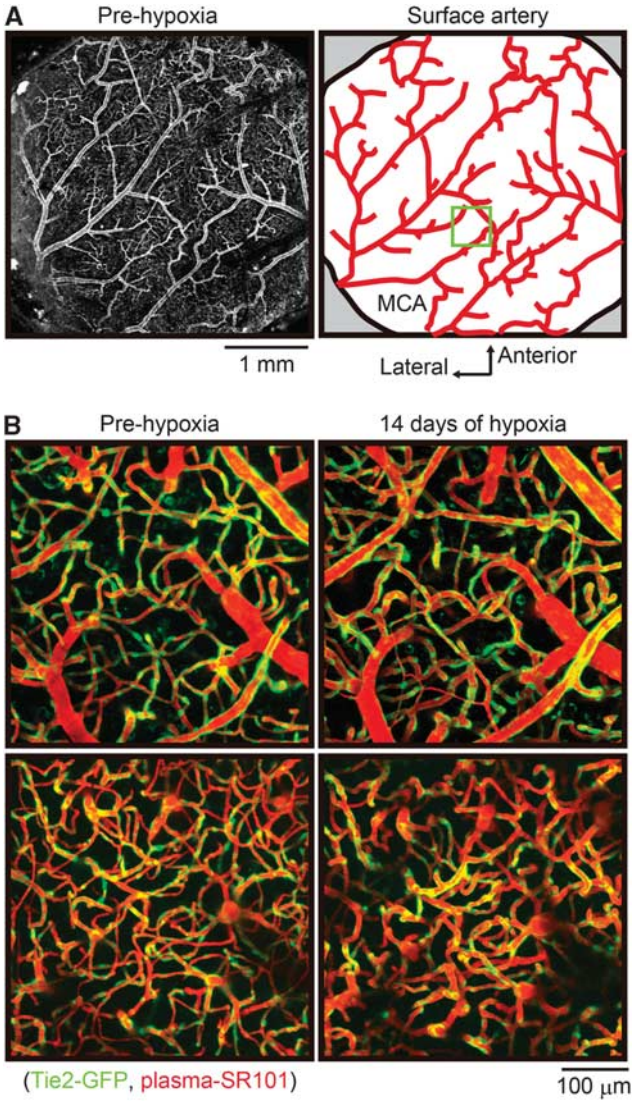

Figure 1. A representative image of the cortical surface and parenchymal vasculature before and after 14 days of hypoxia in a Tie2-green fluorescent protein (GFP) mouse. (**A**) Cortical surface vasculature at prehypoxia. A wide field of view image of GFP-expressing vasculature captured with confocal laser scanning microscopy at prehypoxia (left) was used as a reference to track the target microvessels and astrocytes during the follow-up imaging experiments. The location shown in the green square, a peripheral region of the middle cerebral artery (MCA) territory (right), was imaged using two-photon microscopy (shown in **B**). (**B**) Parenchymal microvessels before (left) and after 14 days of hypoxia (right). The pial arteries (i.e., dense and thick endothelial cells) and veins (i.e., sparse and thin endothelial cells) slightly dilated after 14 days of hypoxia (top right) compared with prehypoxia (top left), whereas the parenchymal capillary diameters drastically increased after 14 days of hypoxia (bottom right) relative to prehypoxia (bottom left). For visual purposes, the image is presented with the maximum intensity projection over depths of 0 to 100 μm (top) and 100 to 300 μm (bottom) from the surface. The red color indicates blood plasma labeled with sulforhodamine 101 (SR101) (plasma-SR101), and green color is GFP-expressing endothelial cells (Tie2-GFP).

Diameter, Cell Volume, and Distance Measurements

All of the images were three-dimensionally reconstructed and analyzed offline using LAS AF software (Leica Microsystems GmbH) or three-dimensional image analysis software (Volocity; Perkin-Elmer Japan, Kanagawa, Japan). The vessel diameter was manually measured at its cross-section between the outer edges of the GFP-expressing endothelial cells. The volume of astrocyte soma was measured after removing the thin processes of the SR101-positive astrocytes in the three-dimensional reconstructed image. The changes of these diameters and cell volumes were compared through prehypoxia with 21 days of hypoxia in the same locations. Five to twenty sections (a total of 52 sections) were randomly selected over depths of 35 to 495 μm from the cortical surface in each animal. For the capillaries positioned in the periartery space ($<$100-μm distance from the penetrating artery), the shortest distance from the wall of the center penetrating artery to its nearest point on the capillary wall was measured (i.e., the shortest distance between the outer edges of the GFP-labeled endothelium of the penetrating artery and the capillary, see Figure 4A). For the astrocytes, a distance between the nearest capillary and the edge of the astrocyte soma was measured to determine the astrocyte migration. The data are represented as the mean $\pm$ standard deviation over the number of animals measured, unless otherwise specified. Statistical significance ($P<0.05$) was examined using Student's *t*-test for comparisons between sprouting and nonsprouting capillary data or Dunnett's test for multiple comparisons with a control (prehypoxia) state across the number of animals.

RESULTS

A representative image shows the identical geometry of the cortical vasculature before and after 14 days of hypoxia (Figure 1B). For the cortical surface vasculature, the preserved pattern was consistently observed in all 11 animals for more than 21 days of hypoxia. A comparison of the individual pial arteries and veins showed a slight increase in their diameters after 14 days of hypoxia compared with prehypoxia (Figure 1B, upper), whereas the parenchymal capillaries showed a drastic increase in their diameters (Figure 1B, lower).

The mean diameter of the center penetrating artery was 18 ± 3, 21 ± 5, 22 ± 6, and 22 ± 6 μm at days 0, 7, 14, and 21 of hypoxia, respectively ($N=5$ animals; Figure 2A), whereas the parenchymal capillary diameters were 4.7 ± 0.6, 6.5 ± 1.0, 6.7 ± 1.6, and 7.3 ± 1.4 μm, respectively ($N=5$; Figure 2A). An approximately 10% decrease in the shortest distance between the center penetrating artery and the nearest capillary was observed after adaptation to chronic hypoxia (Figure 2B). Statistical significance ($P<0.05$) over the five animals measured was detected for the artery–capillary distances after 7 days of hypoxia, and for the parenchymal capillary diameters after 14 and 21 days of hypoxia compared with prehypoxia, but none of the penetrating artery diameters after hypoxia induction.

A total of 45 sprouts were observed in all 11 animals after 7 to 14 days of hypoxia. The head of the sprout had a bump-like shape (Figure 3), and the mean diameter at the greatest width was 14 ± 7 μm (3.6 to 34 μm, $n=45$ sprouts). The inside of the sprout was continuously sealed with GFP-expressing endothelial cells (Supplementary Figure S1), and stagnant blood cells were frequently seen (Supplementary Figure S2 and Supplementary Movie 1). At the place of the sprouting, no predictive morphologic signs were observed for both the endothelial cells and the neighborhood astrocytes. The sprout was mostly located in the upper cortical layers (depths of $\sim$200 μm; Figure 4B). There were no statistically significant correlations between the sprout depth and its diameter ($R=0.24$, $P>0.05$).

More than 50% of the sprouts (24 out of 45 sprouts) were located in the capillaries in the periartery space (Supplementary Figure S1). The capillaries that developed the sprout had a mean shortest distance of 57 ± 17 μm (19 to 89 μm, $n=24$ in 11 animals) from the center penetrating artery, whereas the nonsprouting capillaries had a mean shortest distance of 37 ± 8 μm (19 to 61 μm, $n=71$ in 5 animals; Figure 4C). There were statistically significant differences ($P<0.05$, Student's *t*-test) between the sprouting and nonsprouting capillary to artery distances in the periartery space.

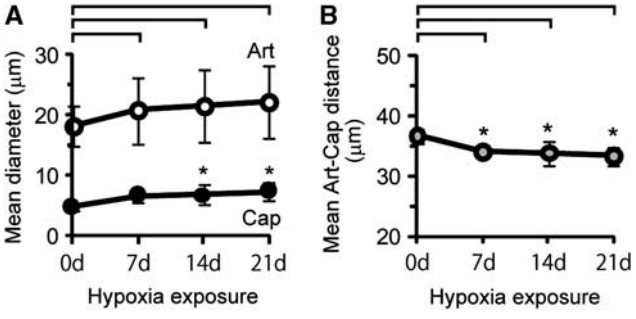

Figure 2. The hypoxia-induced vessel dilation and reduction of shortest distances between the center penetrating arteries and capillaries in the periartery space. (**A**) The mean diameters of the penetrating artery (Art, open circle) and capillaries (Cap, closed circle) from prehypoxia (0d) to 21 days (21d) of hypoxia. *$P<0.05$ (versus prehypoxia). Error bar: standard deviation ($N=5$ animals). (**B**) The mean distance between the wall of the penetrating artery and capillaries for prehypoxia (0d) to 21 days (21d) of hypoxia. *$P<0.05$ (versus prehypoxia). Error bar: standard deviation ($N=5$ animals).

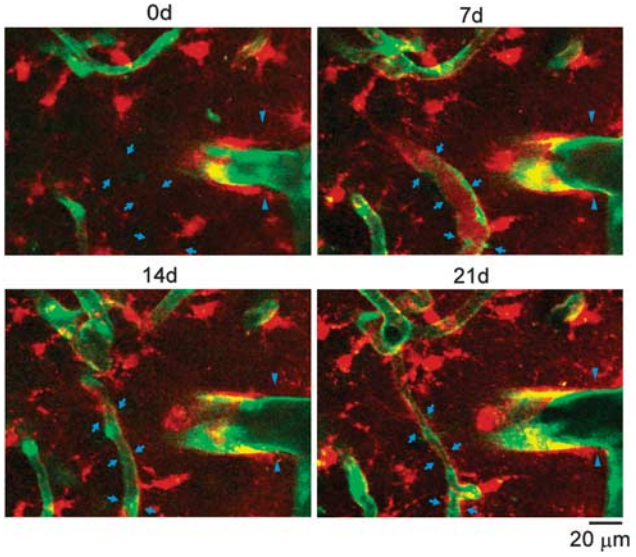

Figure 3. Vessel sprout, extension, and creation of new connection responding to chronic hypoxia. A representative image of the green fluorescent protein (GFP)-expressing endothelial cells (green) and sulforhodamine 101 (SR101)-labeled astrocytes (red), repeatedly imaged over prehypoxia (0d) to 21 days of hypoxia (21d). The new vessel (arrows) appeared at 7 days (7d) of hypoxia in the noncapillary regions around the center penetrating artery (arrowhead, see prehypoxia image), whereas the penetrating artery and parenchymal capillary apparently dilated after 7 days of hypoxia compared with prehypoxia. The newly formed vessel eventually connected with existing capillary (upper side in the image) up to 14 days (14d) of hypoxia. After forming the vessel connection, the shape of the new vessel normalized (i.e., slimed), and no stagnant blood cells were observed. After 14 to 21 days of hypoxia, the new vessel was extensively covered with processes from the neighboring astrocytes. For visual purposes, the maximum intensity projection was performed over depths of 45 to 70 μm from the surface (11 slices).

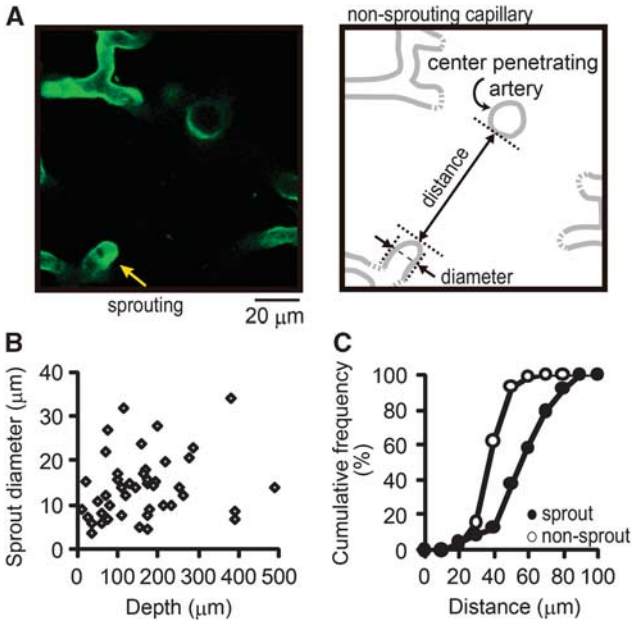

Figure 4. The vessel sprouts and their distances from the center penetrating artery. (**A**) A representative single slice image of the vessel sprout (arrow) appeared in the periartery space at 7 days of hypoxia. The maximum width between the edges of green fluorescent protein (GFP)-expressing endothelial cells was considered to be the diameter of the vessel sprout (right). The shortest distance between the tip of the vessel sprout and the outer edges of the penetrating artery was also measured (right). The penetrating artery and other capillaries (nonsprouting) were continued to upper and lower slices. (**B**) The diameter and depth distribution of the vessel sprouts. A total of 45 sprouts were observed after 7 to 14 days of hypoxia ($N = 11$ animals). No significant correlations ($P > 0.05$) were found between the cortical depth where the sprout appeared over 0 to 500 μm from the surface and their diameters. (**C**) Cumulative frequency for the shortest distance between the center penetrating artery and the sprouting (closed circle) or nonsprouting (open circle) capillaries, observed in the periartery space. The sprouting capillaries were located significantly distant from the center penetrating artery ($P < 0.05$) compared with the nonsprouting capillaries.

In this early phase of hypoxia adaptation (7 to 14 days), no detectable changes in the neighboring astrocyte to the vessel sprout were observed (Supplementary Figure S3, and Supplementary Movies 2 and 3). Nevertheless, most of the sprouts (32 of 45 sprouts) were closely located to large astrocyte processes (Supplementary Figure S1). Repeated imaging further revealed that the sprout extended toward the nonvessel regions while maintaining a bump-like head shape (e.g., 11 day in Supplementary Figure S1), and that 42% of the sprouts (19 of 45 sprouts) became fully connected with an existing capillary up to 21 days of hypoxia (see Figure 5A). However, 9% of the sprouts (4 of 45 sprouts) were pruned within 3 days of its appearance (see Figure 5B). Other 49% of the sprouts were not determined (including the unconnected sprouts and out of the image field) until 21 days of hypoxia. Once the sprout was connected to a recipient capillary, the shape of the new vessel normalized with a diameter similar to the existing capillaries ($\sim 8\,\mu$m), and no stagnant blood cells were observed inside of the vessel (e.g., 14 day in Figure 3).

In the late phase of hypoxia adaptation (14 to 21 days), the newly formed vessel was extensively wrapped with astrocyte processes (Figures 6A and 6B). This adaptation of the neighboring astrocytes followed the formation of the new vessels (see 7 to 21 day in Figure 3). The volume of the astrocyte soma significantly increased: 443 to 573 μm^3 from pre- to 21 days of hypoxia, respectively ($P < 0.05$ for $n = 30$ astrocytes, $N = 2$ animals; Figure 6C). In contrast, there were no statistically significant differences ($P > 0.05$ for $n = 20$ astrocytes) for a distance between the astrocyte soma and the nearest capillaries over the entire periods of hypoxia (Figure 6D). Finally, a leakage of SR101-labeled plasma was not detected for the entire periods of hypoxia experiments in any of the animals (see Figure 3), indicating the preserved integrity of the BBB.

DISCUSSION

The present study characterizes the spatiotemporal dynamics of hypoxia-induced angiogenesis concurrently with morphologic adaptations of the neighboring astrocytes in the adult mouse cortex. The vessel sprout appeared after 7 days of hypoxia from capillaries where no morphologic precursors for endothelial cells and astrocytes were detected. More than 50% of the sprouts were located in the capillaries distant from the center penetrating arteries, indicating a favored site for sprouting. During the later phase of hypoxia adaptation, the newly formed vessel was wrapped with numerous processes from the neighboring astrocytes. This finding indicates that the new vessel provokes the covering of the astrocyte processes to stabilize BBB.

Vascular Sprouting and New Connection

In the cerebral cortex, the periartery space is well-described as a capillary-free zone where oxygen is supplied by the center penetrating artery.[29] Creating a new capillary connection directly approaches the corner of the diffusion limit, and thus the vessel sprout serves to reduce the capillary-free zone effectively. In contrast, the increase in vessel diameter contribute little to reduce the capillary-free zone (10% of prehypoxia conditions; Figure 2B). Under the various concentrations of environmental oxygen, 13%, 21%, 30%, and 40%, a mean width of capillary-free zone was changed as 46, 65, 92, and 104 μm, respectively, in kitten retinas,[30] which indicates the oxygen level-dependent adaptations of the capillary-free zone. In the mouse cortex, the diffusion limit of oxygen from the penetrating artery was 55 and 40 μm under normoxia (21% O_2) and hypoxemia (10% O_2), respectively,[29] whereas the capillaries were 28 and 17 μm, respectively.[29] Namely, it can be expected that a capillary more than 57 μm (40 plus 17 μm) away from the center penetrating artery induces a hypoxic spot between the capillary and the penetrating artery under hypoxia conditions. This estimation reasonably agreed with the results of the mean distances between the artery and capillary that developed the vessel sprouts (Figure 4C).

Three-week hypoxia provoked a 1.6-fold increase in the capillary diameters relative to prehypoxia: 4.7 to 7.3 μm (Figure 2A). The results are in good agreement with our previous report that showed the hypoxia level-dependent increase of the parenchymal capillary diameters under 8% to 9% O_2 (4.9 to 8.5 μm under pre- to 21 days hypoxia, respectively) and 10% to 11% O_2 (5.0 to 6.7 μm under pre- to 21 days hypoxia, respectively).[22] Because these imaging experiments were conducted under 1% isoflurane mixed room air conditions, isoflurane-induced hypoventilation may influence on the vascular diameters. However, capillary dilation responding to hypercapnia is relatively small: 5.3 to 5.7 μm (ref. 31) and 3.7 to 4.1 μm (ref. 32) under normocapinia to hypercapnia, respectively. Therefore, we considered these effects of the hypoventilation were minimal in our experimental conditions. A closed cranial window provided consistent microvessel and astrocyte structures over 2 to 7 weeks after the surgical procedures under normoxia conditions,[21] indicating the minimum effects because of inflammation resulting from the craniotomy. Previous studies for vasodilation to transient hypercapnia[31,32] and

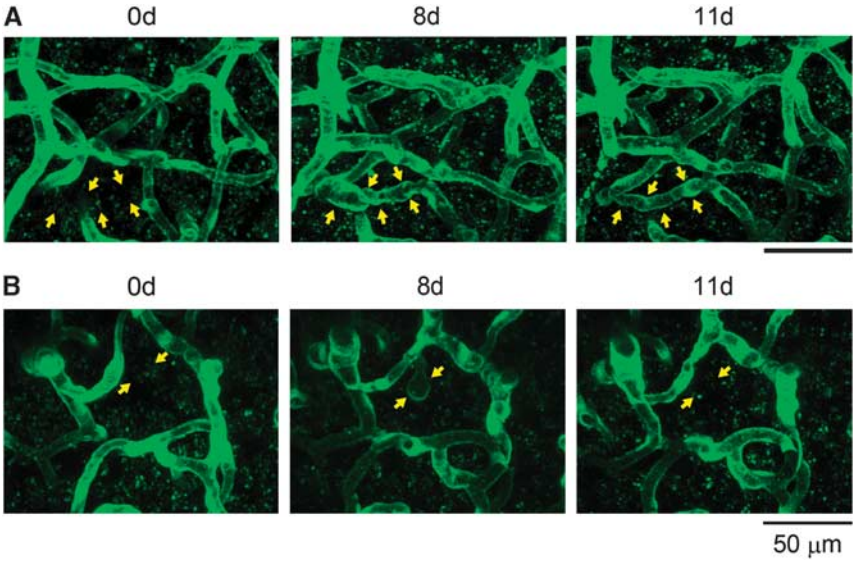

Figure 5. The fate of the vessel sprout. (**A**) A creation of new vessel connection. The sprout (arrows) connected with an existing capillary after 8 days (8d) of hypoxia (center). After 11 days (11d) of hypoxia, the shape of this newly formed vessel becomes normalized, similar to the other existing capillaries (right). Note that a lumen of the new vessel was completely sealed with green fluorescent protein (GFP)-expressing endothelial cells. (**B**) An elimination of the sprout. The sprout (arrows) observed after 8 days of hypoxia (center) was eliminated after 11 days of hypoxia (right). For visual purposes, the images are shown as the maximum intensity projection.

neural activation[33,34] showed that the diameter of the parenchymal capillary was relatively stable, with at most a 10% change. Thus, the mechanism of vasodilation induced through chronic hypoxia differs from the previously known responses. In *in vitro* experiments, a lower oxygen concentration (5% O_2) provoked the greatest proliferative response in vascular endothelial cells.[35] This indicates that the hypoxia used in the present experiments (8% to 9% O_2) could be low enough to trigger proliferative responses in the vascular endothelial cells.

Nevertheless, 9% of the sprouts were eliminated shortly after their emergences (Figure 5B), whereas a regression of the existing vessels was not detected. A previous study showed that chronic mild hypoxia (10% O_2) induced a fivefold increase in vessel formation but no difference in elimination between hypoxia- and normoxia-treated mice.[14] The discrepancy between the previous and the present studies could be because of a difference in the methodology and/or experimental conditions. In the present experiment, the cerebral vasculature was visualized for the both GFP-expressing endothelium and SR101-labeled plasma, and the pruning of the vessel sprouts was determined based on a loss of GFP-expressing endothelial cells. By using only a plasma-labeling technique, an occasional closure of narrow capillaries, which has not been seen in normal brains, cannot be completely ruled out. The factors that determine the fate of the sprout are beyond the scope of the present study. Maintaining extension of the vessel sprout may require persistent expression of growth factors (e.g., vascular endothelial growth factor and angiopoietin-2). Significant increases of the brain hypoxia-inducible factor-1α expression are detected below 12% O_2 for minimum 4 hours exposures.[36] The maximal 9- to 10-fold increase of the hypoxia-inducible factor-1α protein levels were also reported for 6 hours to 4 days of hypoxia (10% O_2).[8] However, the increased hypoxia-inducible factor-1α protein levels eventually returned to the level of normoxic conditions up to 21 days of hypoxia adaptations.[8] Similarly, vascular endothelial growth factor protein expression was upregulated for only early phase of the hypoxia adaptation (1 to 7 days) but returned to the normoxia level after 21 days of chronic hypoxia.[9] In contrast, prolonged upregulation was found for angiopoietin-2 expression during 6 hours to 14 days of chronic hypoxia (10% O_2).[10] These temporal dynamics of the molecular expressions and their localizations in relation to a place of the sprouting should be identified in future works.

Morphologic Adaptation of Neighboring Astrocytes with Preserved Blood–Brain Barrier Integrity

The newly formed vessels were extensively wrapped with the neighboring astrocyte processes after vessel formation during the late phase of hypoxia adaptation (Figure 6). In contrast, detectable changes in the astrocyte processes were not observed during early phases of hypoxia (Supplementary Figure S3), although changes of the thin processes that were not visible using the current methods cannot be ruled out. The temporal dynamics of the astrocyte responses to chronic hypoxia are in good agreement with the previous report that showed the enhanced expression of astrocyte endfoot adhesion molecules (e.g., $\alpha 6\beta 4$ integrin and dystroglycan) for the later phases of hypoxia adaptation.[18] A potential mechanism responsible for the astrocyte adaptation could be therefore that (1) an immature vessel releases some guiding factors that promote the covering of the astrocyte processes and/or (2) a thin process of the astrocyte surveys the immature vessels. Over 21 days of hypoxia, no detectable leakage of the SR101-labeled plasma was observed. In addition, we ensured no leakage of intraperitoneally injected Evans blue (4% in saline) in hypoxia adaptation mouse cortex (Supplementary Figure S4). These findings therefore show that integrity of the BBB is maintained for hypoxia-induced cerebral angiogenesis irrespective of the degree of astrocytic covering.

Mechanistic Insights for the Cellular Interplay of Neuron–Glia–Vascular Units during Cerebral Angiogenesis

Because our results showed the preserved integrity of the BBB including the early phase of hypoxia adaptation where astrocyte morphology remains unchanged, other cellular mechanisms, such as by pericytes, may also contribute to the angiogenic responses. Pericyte, which shares a common basement membrane with endothelial cells, has a crucial role in stabilizing the immature vessels,[37,38] and maintaining the functional integrity of the

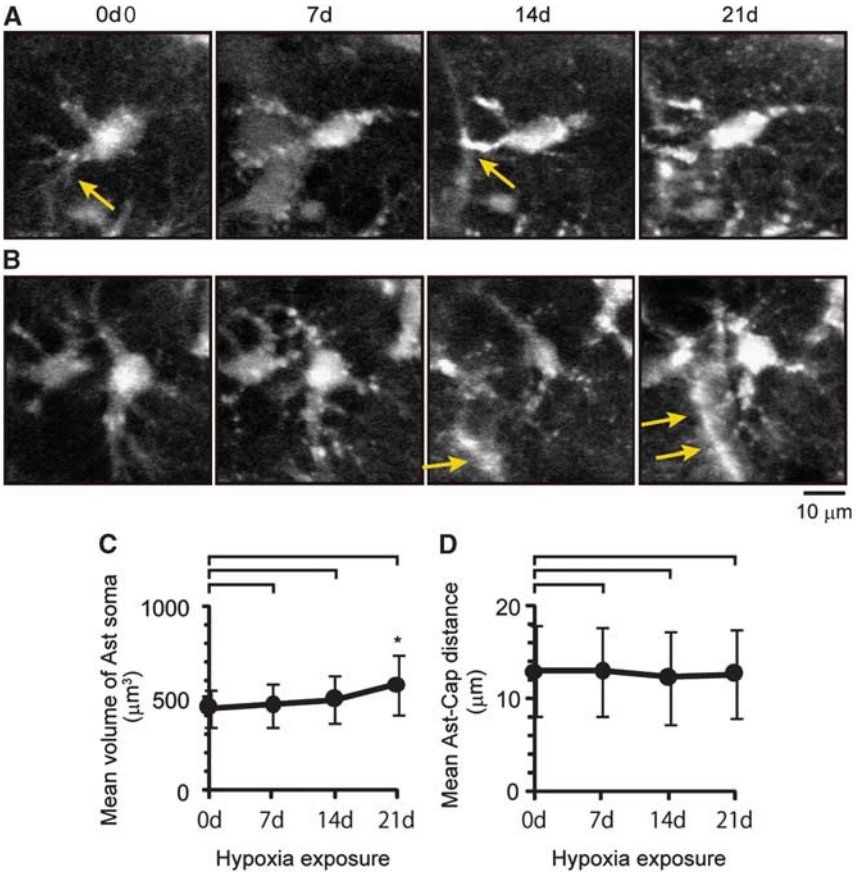

Figure 6. Morphologic adaptations of the neighboring astrocytes. (**A**) Morphologic changes in astrocytes near the new vessels (a gray scale indicates an intensity of sulforhodamine 101 (SR101) label). One of the processes (indicated as arrow) of the neighboring astrocyte touches the outer wall of the new vessel after 14 days of hypoxia after the arrival of the new vessel. (**B**) Morphologic changes in astrocytes around the connection point. The numerous processes of the neighboring astrocytes extend to the newly formed vessel (arrows) during 14 to 21 days of hypoxia. For visual purposes, these images show the maximum intensity projection at depths of 8 to 16 μm from the surface (i.e., three slices). (**C**) The mean volume of the astrocyte soma from prehypoxia (0d) to 21 days of hypoxia (21d). *$P < 0.05$ (versus prehypoxia, $n = 30$ astrocytes). Error bar: standard deviation ($n = 30$ in 2 animals). (**D**) The mean distance between the nearest capillary (Cap) and astrocyte soma (Ast). No statistically significant change was observed for the entire periods of hypoxia ($P > 0.05$, versus prehypoxia, $n = 20$ astrocytes), indicating the no migration of the astrocyte soma, but their processes were extended. Error bar: standard deviation ($n = 20$ in 2 animals).

BBB.[39,40] Thus, pericyte–endothelial cell interactions must have a role in maintaining the BBB integrity and normalization of the vasculature during adaptation to chronic hypoxia. However, little is known about the involvement of the pericytes in the process of cerebral angiogenesis responding to hypoxia. Using β-actin-GFP transgenic mouse line, Fernández–Klett showed that pericytes can be visualized *in vivo* under two-photon microscopy.[41] Thus, the dynamic changes of the pericytes can be tracked *in vivo* during hypoxia-induced cerebral angiogenesis.

In addition to the present results, we also observed no detectable sprouting for 4 days of hypoxia or 3 months of normoxia (data not shown). These findings therefore indicate that hypoxia-induced angiogenesis takes approximately 1 week to create a vessel sprout and further 1 week to make a new connection and blood flow. This time delay behind the onset of hypoxia events should be improved to promote angiogenesis for the treatment of the hypoxic/ischemic tissue, because the sprouting, extension, and creation of new vessel connections are needed to restore immediately the hypoxic/ischemic tissue. Multidimensional (space and time) live cell imaging to explore the chronic phase of cellular interplays, as presented here, would further unveil the central mechanism that promotes cerebral angiogenesis and maintains a functional BBB in health and disease brains.

CONCLUSION

Hypoxia-induced cerebral angiogenesis provokes the covering of the neighborhood astrocyte processes, which may stabilize BBB integrity in immature vessels. Because this adaptive mechanism is critical for protecting and strengthening the 'neuron–glia–vascular unit', as in neurodegenerative disorders, future works are needed to further examine the molecular mechanism for the interactions of astrocyte processes and vascular endothelial cells responding to chronic hypoxia.

DISCLOSURE/CONFLICT OF INTEREST

The authors declare no conflict of interest.

REFERENCES

1 Mathiisen TM, Lehre KP, Danbolt NC, Ottersen OP. The perivascular astroglial sheath provides a complete covering of the brain microvessels: an electron microscopic 3D reconstruction. *Glia* 2010; **58**: 1094–1103.
2 Abbott NJ, Patabendige AA, Dolman DE, Yusof SR, Begley DJ. Structure and function of the blood–brain barrier. *Neurobiol Dis* 2010; **37**: 13–25.
3 Ujiie M, Dickstein DL, Carlow DA, Jefferies WA. Blood–brain barrier permeability precedes senile plaque formation in an Alzheimer disease model. *Microcirculation* 2003; **10**: 463–470.

4 Rigau V, Morin M, Rousset MC, de Bock F, Lebrun A, Coubes P *et al.* Angiogenesis is associated with blood–brain barrier permeability in temporal lobe epilepsy. *Brain* 2007; **130**: 1942–1956.
5 Zacchigna S, Lambrechts D, Carmeliet P. Neurovascular signalling defects in neurodegeneration. *Nat Rev Neurosci* 2008; **9**: 169–181.
6 Carvey PM, Hendey B, Monahan AJ. The blood–brain barrier in neurodegenerative disease: a rhetorical perspective. *J Neurochem* 2009; **111**: 291–314.
7 Zlokovic BV. Neurovascular pathways to neurodegeneration in Alzheimer's disease and other disorders. *Nat Rev Neurosci* 2011; **12**: 723–738.
8 Chávez JC, Agani F, Pichiule P, LaManna JC. Expression of hypoxia-inducible factor-1alpha in the brain of rats during chronic hypoxia. *J Appl Physiol* 2000; **89**: 1937–1942.
9 Kuo NT, Benhayon D, Przybylski RJ, Martin RJ, LaManna JC. Prolonged hypoxia increases vascular endothelial growth factor mRNA and protein in adult mouse brain. *J Appl Physiol* 1999; **86**: 260–264.
10 Pichiule P, LaManna JC. Angiopoietin-2 and rat brain capillary remodeling during adaptation and deadaptation to prolonged mild hypoxia. *J Appl Physiol* 2002; **93**: 1131–1139.
11 Milner R, Hung S, Erokwu B, Dore-Duffy P, LaManna JC, del Zoppo GJ. Increased expression of fibronectin and the alpha 5 beta 1 integrin in angiogenic cerebral blood vessels of mice subject to hypobaric hypoxia. *Mol Cell Neurosci* 2008; **38**: 43–52.
12 LaManna JC, Vendel LM, Farrell RM. Brain adaptation to chronic hypobaric hypoxia in rats. *J Appl Physiol* 1992; **72**: 2238–2243.
13 Boero JA, Ascher J, Arregui A, Rovainen C, Woolsey TA. Increased brain capillaries in chronic hypoxia. *J Appl Physiol* 1999; **86**: 1211–1219.
14 Harb R, Whiteus C, Freitas C, Grutzendler J. *In vivo* imaging of cerebral microvascular plasticity from birth to death. *J Cereb Blood Flow Metab* 2013; **33**: 146–156.
15 Herbert SP, Stainier DY. Molecular control of endothelial cell behaviour during blood vessel morphogenesis. *Nat Rev Mol Cell Biol* 2011; **12**: 551–564.
16 Coulon C, Georgiadou M, Roncal C, De Bock K, Langenberg T, Carmeliet P. From vessel sprouting to normalization: role of the prolyl hydroxylase domain protein/hypoxia-inducible factor oxygen-sensing machinery. *Arterioscler Thromb Vasc Biol* 2010; **30**: 2331–2336.
17 Eilken HM, Adams RH. Dynamics of endothelial cell behavior in sprouting angiogenesis. *Curr Opin Cell Biol* 2010; **22**: 617–625.
18 Li L, Welser JV, Dore-Duffy P, del Zoppo GJ, Lamanna JC, Milner R. In the hypoxic central nervous system, endothelial cell proliferation is followed by astrocyte activation, proliferation, and increased expression of the alpha 6 beta 4 integrin and dystroglycan. *Glia* 2010; **58**: 1157–1167.
19 Tam SJ, Watts RJ. Connecting vascular and nervous system development: angiogenesis and the blood–brain barrier. *Annu Rev Neurosci* 2010; **33**: 379–408.
20 Tomita Y, Kubis N, Calando Y, Tran Dinh A, Méric P, Seylaz J *et al.* Long-term *in vivo* investigation of mouse cerebral microcirculation by fluorescence confocal microscopy in the area of focal ischemia. *J Cereb Blood Flow Metab* 2005; **25**: 858–867.
21 Masamoto K, Tomita Y, Toriumi H, Aoki I, Unekawa M, Takuwa H *et al.* Repeated longitudinal *in vivo* imaging of neuro-glio-vascular unit at the peripheral boundary of ischemia in mouse cerebral cortex. *Neuroscience* 2012; **212**: 190–200.
22 Yoshihara K, Takuwa H, Kanno I, Okawa S, Yamada Y, Masamoto K. 3D analysis of intracortical microvasculature during chronic hypoxia in mouse brains. *Adv Exp Med Biol* 2013; **765**: 357–363.
23 Motoike T, Loughna S, Perens E, Roman BL, Liao W, Chau TC *et al.* Universal GFP reporter for the study of vascular development. *Genesis* 2000; **28**: 75–81.
24 Itoh Y, Toriumi H, Yamada S, Hoshino H, Suzuki N. Resident endothelial cells surrounding damaged arterial endothelium reendothelialize the lesion. *Arterioscler Thromb Vasc Biol* 2010; **30**: 1725–1732.
25 Nimmerjahn A, Kirchhoff F, Kerr JN, Helmchen F. Sulforhodamine 101 as a specific marker of astroglia in the neocortex *in vivo*. *Nat Methods* 2004; **1**: 31–37.
26 Takuwa H, Autio J, Nakayama H, Matsuura T, Obata T, Okada E *et al.* Reproducibility and variance of a stimulation-induced hemodynamic response in barrel cortex of awake behaving mice. *Brain Res* 2011; **1369**: 103–111.
27 Takuwa H, Masamoto K, Yamazaki K, Kawaguchi H, Ikoma Y, Tajima Y *et al.* Long-term adaptation of cerebral hemodynamic response to somatosensory stimulation during chronic hypoxia in awake mice. *J Cereb Blood Flow Metab* 2013; **33**: 774–779.
28 Kasischke KA, Lambert EM, Panepento B, Sun A, Gelbard HA, Burgess RW *et al.* Two-photon NADH imaging exposes boundaries of oxygen diffusion in cortical vascular supply regions. *J Cereb Blood Flow Metab* 2011; **31**: 68–81.
29 Phelps DL. Oxygen and developmental retinal capillary remodeling in the kitten. *Invest Ophthalmol Vis Sci* 1990; **31**: 2194–2200.
30 Villringer A, Them A, Lindauer U, Einhäupl K, Dirnagl U. Capillary perfusion of the rat brain cortex. An *in vivo* confocal microscopy study. *Circ Res* 1994; **75**: 55–62.
31 Hutchinson EB, Stefanovic B, Koretsky AP, Silva AC. Spatial flow-volume dissociation of the cerebral microcirculatory response to mild hypercapnia. *NeuroImage* 2006; **32**: 520–530.
32 Stefanovic B, Hutchinson E, Yakovleva V, Schram V, Russell JT, Belluscio L *et al.* Functional reactivity of cerebral capillaries. *J Cereb Blood Flow Metab* 2008; **28**: 961–972.
33 Drew PJ, Shih AY, Kleinfeld D. Fluctuating and sensory-induced vasodynamics in rodent cortex extend arteriole capacity. *Proc Natl Acad Sci USA* 2011; **108**: 8473–8478.
34 Rosen P, Boulton M, Moriarty P, Khaliq A, McLeod D. Effect of varying oxygen concentrations on the proliferation of retinal microvascular cells *in vitro*. *Exp Eye Res* 1991; **53**: 597–601.
35 Chavez JC, LaManna JC. Activation of hypoxia-inducible factor-1 in the rat cerebral cortex after transient global ischemia: potential role of insulin-like growth factor-1. *J Neurosci* 2002; **22**: 8922–8931.
36 Vérant P, Serduc R, van der Sanden B, Chantal R, Ricard C, Coles JA *et al.* Subtraction method for intravital two-photon microscopy: intraparenchymal imaging and quantification of extravasation in mouse brain cortex. *J Biomed Opt* 2008; **13**: 011002.
37 Winkler EA, Bell RD, Zlokovic BV. Central nervous system pericytes in health and disease. *Nat Neurosci* 2011; **14**: 1398–1405.
38 Darland DC, Massingham LJ, Smith SR, Piek E, Saint-Geniez M, D'Amore PA. Pericyte production of cell-associated VEGF is differentiation-dependent and is associated with endothelial survival. *Dev Biol* 2003; **264**: 275–288.
39 Armulik A, Genové G, Mäe M, Nisancioglu MH, Wallgard E, Niaudet C *et al.* Pericytes regulate the blood–brain barrier. *Nature* 2010; **468**: 557–561.
40 Daneman R, Zhou L, Kebede AA, Barres BA. Pericytes are required for blood–brain barrier integrity during embryogenesis. *Nature* 2010; **468**: 562–566.
41 Fernández-Klett F, Offenhauser N, Dirnagl U, Priller J, Lindauer U. Pericytes in capillaries are contractile in vivo, but arterioles mediate functional hyperemia in the mouse brain. *Proc Natl Acad Sci USA* 2010; **107**: 22290–22295.

Supplementary Information accompanies the paper on the Journal of Cerebral Blood Flow & Metabolism website (http://www.nature.com/jcbfm)